

# Velocity-Based Variable Thresholds for Improving Collision Detection in Manipulators\*

Vahid Sotoudehnejad<sup>1</sup> and Mehrdad R. Kermani<sup>2</sup>

**Abstract**—In absence of tactile and visual sensors, manipulators rely on dynamic modeling and force/torque sensors to detect collisions. Predicated upon the understanding that collision detection will be improved by removing the effects of torque sensor error and friction compensation error, we propose an approach to measure these undesired effects in external torque residual signals without resorting to remodeling of the robot. Compensation of these effects leads to the proposed velocity-based variable thresholds which are shown to detect collisions with better efficacy than uncompensated methods. Implementation of the proposed velocity-based variable thresholds on a torque sensor equipped robot validates our methodology.

## I. INTRODUCTION

When robots and humans share a common space, immediate removal of collisions is crucial to the human safety. Accurate collision detection ensures that active post-collision strategies, which are designed to prevent injuries to humans, are employed as soon as possible. Collisions can either be detected with or without tactile sensors. Considering the cost and the size of tactile sensors, it is more favourable if the robot is able to detect collisions without such sensors. The use of force/torque sensors in robot joints is an alternative solution. The most cost effective method is to use force/torque residual observers to estimate external torques exerted on the robot by the environment. Several observer-based methods without using torque sensors have been proposed to obtain external torques [5], [6], [7], [8], [9]. The implementation of high gain observers [8], for estimating external torques in manipulators was proposed in [9] and is used in this paper for the calculation of external torque residuals.

This paper describes how collision detection in manipulators can be improved if the dynamic modeling errors, friction compensation errors and sensor errors were taken into consideration. We propose techniques for finding estimations of modeling and sensor errors without resorting to complete remodeling of the robot. The proposed techniques are developed for robots with and without joint torque sensors and used to introduce velocity-based variable thresholds. It is shown that by compensating the torque residual thresholds with the velocity-based variable thresholds, collisions can

\*This work was supported by the Natural Sciences and Engineering Research Council (NSERC) of Canada under Grant RGPIN 346166 and Ontario Centres of Excellence (OCE) under Grant MR 90545.

<sup>1</sup>V. Sotoudehnejad is with the Department of Electrical and Computer Engineering, the University of Western Ontario, London, Canada, N6A 5B9 vsotoude@uwo.ca

<sup>2</sup>M. R. Kermani is with the Department of Electrical and Computer Engineering, the University of Western Ontario, London, Canada, N6A 5B9, and also with the Canadian Surgical Technologies and Advanced Robotics (CSTAR) Research Centre, London Health Sciences Centre, London, Canada, N6A 5A5 mkermani@eng.uwo.ca

be detected more accurately compared to uncompensated thresholds.

The organization of this paper is as follows. Section II covers manipulator modeling equations and external torque observers with and without joint torque sensors. Section III analyzes the effects of inaccurate modeling and torque sensor errors on external torque observers. In section IV, velocity-based variable thresholds for collision detection are proposed. In section V, the proposed velocity-based thresholds are implemented on the torque sensor equipped KUKA-LWR. Collision detection capability of the proposed thresholds is compared to those obtained from uncompensated thresholds on the KUKA-LWR. Section VI concludes the paper.

## II. MANIPULATOR MODELING AND CALCULATION OF EXTERNAL TORQUES

A manipulator's dynamic equation is given by,

$$M(q)\ddot{q} + C(q, \dot{q})\dot{q} + g(q) = \tau_m + \tau_d + \tau_c - \tau_{fr} \quad (1)$$

where  $q$  denotes the joint position,  $M(q)$  is the inertia matrix,  $C(q, \dot{q})$  is the centrifugal and Coriolis matrix, and  $g(q)$  is the gravitational vector. Also  $\tau_m$  represents the motor torque,  $\tau_{fr}$  is the friction torque,  $\tau_d$  represents disturbance torque, and  $\tau_c$  represents external torques acting on the manipulator. In this section, two methods for observing external torques with and without torque sensors are discussed.

### A. External Torque Observer Using Motor Torques

Various external torque observers have been used in the literature, including high gain observers and sliding mode observers [8], observers based on adaptive control law [10], and nonlinear disturbance observers [7]. A common drawback of these observers is their complex dynamics, which in case of error analyses leads to further complications. In this paper, we use the observer discussed in [9] which provides a simple first-order estimation of external torques. The observer is defined using the generalized momentum of the robot i.e.,

$$p(t) = M(q)\dot{q} \quad (2)$$

and is equal to the following N-dimensional residual for the external torques  $\tau_c$ ,

$$r(t) = K_I \left[ p(t) - \int_0^t (\tau_m + \tau_d + C^T(q, \dot{q})\dot{q} - g(q) - \tau_{fr} + r) du - p(0) \right] \quad (3)$$

where  $N$  is the number of robot joints, and  $K_I$  is the observer gain. In (3),  $r(t)$  represents the first-order filtered value

of  $\tau_c$  [9], i.e.  $r(t) = K_I \tau_c / (s + K_I)$ , where  $s$  represents the Laplace transform. Accurate calculation of  $r(t)$  is not possible due to errors in dynamic modeling, joint flexibility, friction modeling, sensor readings, and disturbance torques  $\tau_d$ . Hence, one is limited to,

$$\hat{r}(t) = K_I \left[ \hat{p}(t) - \int_0^t (\hat{\tau}_m + \hat{C}^T(\hat{q}, \hat{\dot{q}})\hat{\dot{q}} - \hat{g}(\hat{q}) - \hat{\tau}_{fr} + \hat{r}) du - \hat{p}(0) \right] \quad (4)$$

where the hatted values are the approximations obtained through either modeling, online calculations, or real-time sensor readings. The solution of the differential equation (4) with respect to  $\hat{r}(t)$  is given by,

$$\begin{aligned} \hat{r}(t) &= K_I \left[ \hat{p}(t) - K_I (e^{-K_I t} * \hat{p}(t)) \right] \\ &- K_I \left( e^{-K_I t} * (\hat{\tau}_m + \hat{C}^T(\hat{q}, \hat{\dot{q}})\hat{\dot{q}} - \hat{g}(\hat{q}) - \hat{\tau}_{fr}) \right) \end{aligned} \quad (5)$$

where  $*$  denotes convolution. The initial value  $\hat{p}(0)$  has only a transient effect on  $\hat{r}(t)$  and is ignored in (5). The external torque residual in equation (4) is approximately zero as long as there is no collision [9], i.e.,

$$\tau_c(t) = 0 \implies \hat{r}(t) \approx 0 \quad (6)$$

In order to use  $\hat{r}(t)$  for detecting collisions, the simplest method is to choose a threshold  $b$  for  $\hat{r}(t)$  so that upon exceeding this threshold, i.e.,  $|\hat{r}(t)| > b$ , post-collision routines are triggered.

#### B. Measuring External Torques Using Joint Torque Sensors

Availability of force/torque sensors in robot joints provides another method for measuring external torques. These sensors measure the sum of external forces/torques and manipulator dynamics, i.e.,

$$\tau_s = M_s(q)\ddot{q} + C_s(q, \dot{q})\dot{q} + g_s(q) - \tau_{d_s} - \tau_c + \tau_{fr_L} \quad (7)$$

where the subscript  $s$  denotes the parameters as measured from the location of the torque sensors, and  $\tau_{d_s}$  is the disturbance torque on the torque sensors. To avoid using the estimated values of joint accelerations to calculate  $\tau_c$ , an observer similar to (3) can be used,

$$\begin{aligned} r_s(t) &= K_I \left[ p_s(t) - \int_0^t (\tau_s + \tau_{d_s} + C_s^T(q, \dot{q})\dot{q} - g_s(q) - \tau_{fr_L} + r_s) du - p_s(0) \right] \end{aligned} \quad (8)$$

Similar to (4), using available estimations, the corresponding observer for  $\hat{\tau}_c$  is given by,

$$\begin{aligned} \hat{r}_s(t) &= K_I \left[ \hat{p}_s(t) - \int_0^t (\hat{\tau}_s + \hat{C}_s^T(\hat{q}, \hat{\dot{q}})\hat{\dot{q}} - \hat{g}_s(\hat{q}) - \hat{\tau}_{fr_L} + \hat{r}_s) du - \hat{p}_s(0) \right] \end{aligned} \quad (9)$$

In the same manner as (5), the solution to (9) with respect to  $\hat{r}_s$  is given by,

$$\begin{aligned} \hat{r}_s(t) &= K_I \left[ \hat{p}_s(t) - K_I (e^{-K_I t} * \hat{p}_s(t)) \right] \\ &- K_I \left( e^{-K_I t} * (\hat{\tau}_s + \hat{C}_s^T(\hat{q}, \hat{\dot{q}})\hat{\dot{q}} - \hat{g}_s - \hat{\tau}_{fr_L}) \right) \end{aligned} \quad (10)$$

The accuracy of the observers (4), and (9) is prone to modeling and measurement errors.

### III. EFFECTS OF UNMODELED DYNAMICS ON MEASURING EXTERNAL TORQUES

Unmodeled dynamics appear in the calculation of external torques. In this section, the effects of such dynamics on the torque observer are examined and approaches for minimizing their impact on external torque measurements are presented. The formulation of unmodeled dynamics provided in this section will be used in Section IV to define velocity-based variable thresholds.

#### A. Motor Torque Observer

The effect of inaccurate modeling on the external torque observer is defined as the difference between the actual external torques and the observed external torques, i.e.,

$$\tilde{r}(t) = \hat{r}(t) - r(t) \quad (11)$$

where  $\tilde{r}(t)$  can be obtained in the same way described for  $\hat{r}(t)$  in (5),

$$\begin{aligned} \tilde{r}(t) &= K_I \left[ \tilde{p}(t) - K_I (e^{-K_I t} * \tilde{p}(t)) \right] \\ &- K_I \left( e^{-K_I t} * (\tilde{\tau}_m - \tau_d + \tilde{v} - \tilde{g} - \tilde{\tau}_{fr}) \right) \end{aligned} \quad (12)$$

in that  $\tilde{\tau}_m = \hat{\tau}_m - \tau_m$ ,  $\tilde{p}(t) = \hat{M}(\hat{q})\hat{\dot{q}} - M(q)\dot{q}$ ,  $\tilde{v}(t) = \hat{C}^T(\hat{q}, \hat{\dot{q}})\hat{\dot{q}} - C^T(q, \dot{q})\dot{q}$ ,  $\tilde{g}(t) = \hat{g}(\hat{q}) - g(q)$ , and  $\tilde{\tau}_{fr} = \hat{\tau}_{fr} - \tau_{fr}$ . Here we define two terms that contribute to (12) and come from modeling inaccuracies. First term is due to the friction modeling error and the inaccuracy in estimating controlled motor torques,

$$\tau_{fme} = \tilde{\tau}_{fr} - \tilde{\tau}_m \quad (13)$$

The second term is the effects of dynamic modeling error in (12),

$$\begin{aligned} \tilde{h}(t) &\triangleq K_I \left[ \tilde{p}(t) - K_I (e^{-K_I t} * \tilde{p}(t)) \right] \\ &- K_I \left( e^{-K_I t} * (\tilde{v} - \tilde{g}) \right) \end{aligned} \quad (14)$$

The problem of improving the external torque observer  $\hat{r}(t)$  is equivalent to the problem of estimating or minimizing  $\tau_{fme}(t)$  and  $\tilde{h}(t)$ . This paper will propose velocity-based variable thresholds to reduce the effects of  $\tau_{fme}(t)$  and  $\tilde{h}(t)$  on collision detection outcomes obtained from the external torque observer  $\hat{r}(t)$ . In the next section, the suitability of employing joint torque sensors in reducing the effects of inaccurate modeling is studied.

#### B. Joint Torque Sensor Observer

When torque sensors are employed for the calculation of external torques, the effect of measurement and modeling errors in the external torque residual is the difference between (9) and (8), i.e.,

$$\tilde{r}_s(t) = \hat{r}_s(t) - r_s(t) \quad (15)$$

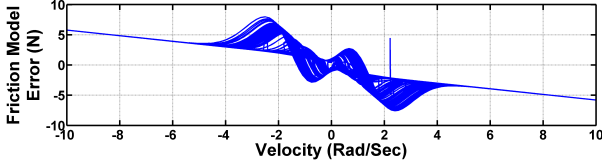


Fig. 1: Simulated values of friction estimation error for a LuGre model with 15% parameter uncertainty

Consequently, similar to (12),  $\tilde{r}_s(t)$  can be expressed as,

$$\begin{aligned} \tilde{r}_s(t) &= K_I \left[ \tilde{p}_s(t) - K_I (e^{-K_I t} * \tilde{p}_s(t)) \right] \\ &- K_I (e^{-K_I t} * (\tilde{\tau}_s - \tau_{d_s} + \tilde{v}_s - \tilde{g}_s - \tilde{\tau}_{fr_L})) \end{aligned} \quad (16)$$

where  $\tilde{\tau}_s = \hat{\tau}_s - \tau_s$ ,  $\tilde{p}_s = \hat{p}_s - p_s$ ,  $\tilde{v}_s = \hat{v}_s - v_s$ ,  $\tilde{g}_s = \hat{g}_s - g_s$ , and  $\tilde{\tau}_{fr_L} = \hat{\tau}_{fr_L} - \tau_{fr_L}$ . In the manner of (14) and (13), the following two term contribute to (16) and come from modeling inaccuracies,

$$\tau_{sf_e} = \tilde{\tau}_s - \tilde{\tau}_{fr_L} \quad (17)$$

$$\begin{aligned} \tilde{h}_s(t) &= K_I \left[ \tilde{p}_s(t) - K_I (e^{-K_I t} * \tilde{p}_s(t)) \right] \\ &- K_I (e^{-K_I t} * (\tilde{v}_s - \tilde{g}_s)) \end{aligned} \quad (18)$$

In the next section, we propose the velocity-based variable thresholds for collision detection by exploiting the inaccuracies of  $\hat{\tau}_{sf_e}$  and  $\hat{\tau}_{fme}$ , and using the approximations of  $\hat{h}(t)$  and  $\hat{h}_s(t)$ . To this effect, we employ the formulation of the unmodeled dynamics of manipulators provided above.

#### IV. VELOCITY-BASED VARIABLE THRESHOLDS FOR COLLISION DETECTION

First, we analyze the effects of inaccurate friction modeling on collision detection thresholds. Given that most friction models, e.g. LuGre model, are velocity dependent, inaccurate modeling of friction results in velocity-dependent errors. To delineate this matter, the effects of parameter uncertainty on the LuGre model, as defined in [12], is explored here via simulations. A Monte Carlo simulation on a LuGre friction model with a maximum of 15% uncertainty for all of its parameters is performed. The input to the LuGre model were 500 fourth order polynomial velocity trajectories of different lengths throughout a total time span of 1000 seconds. Fig. 1 shows the results of this simulation, i.e.  $\tilde{\tau}_{fr} = \hat{\tau}_{fr} - \tau_{fr}$ . From Fig. 1, it is clear that the friction modeling error  $|\tilde{\tau}_{fr}| = |\hat{\tau}_{fr} - \tau_{fr}|$  is dependent on the velocity, i.e.

$$|\tilde{\tau}_{fr}(t)| \leq \beta(\dot{q}) \quad (19)$$

$$\beta(\dot{q}_0) = \max_t |\tilde{\tau}_{fr}(t)|, \quad \forall \dot{q}(t) = \dot{q}_0 \quad (20)$$

Thereby for any mechanical system with friction, including manipulators, it can be safely assumed that a function  $\beta(\dot{q})$  exists that determines the maximum friction modeling error at any given velocity. This concept will later be used for determination of the velocity-based variable thresholds. Also, in case of position-based friction models, the joint positions can be used as independent variables for determination of  $\beta$ .

The second step in determining the collision detection thresholds is considering the unmodeled dynamics. For the velocity-based variable thresholds, we use an approximation of  $\tilde{h}(t)$  and  $\tilde{h}_s(t)$  introduced in [13]. This approximation is based on the different joint-by-joint effects of the uncertainty in the model of the physical parameters of the robot in estimation of external torques. These approximations are

$$\tilde{h}(t) \approx \gamma \hat{h}(t) \quad (21)$$

$$\begin{aligned} \hat{h}(t) &\triangleq K_I \left[ \hat{p}(t) - K_I (e^{-K_I t} * \hat{p}(t)) \right] \\ &- K_I (e^{-K_I t} * (\hat{v} - \hat{g})) \end{aligned} \quad (22)$$

$$\tilde{h}_s(t) \approx \gamma_s \hat{h}_s(t) \quad (23)$$

$$\begin{aligned} \hat{h}_s(t) &\triangleq K_I \left[ \hat{p}_s(t) - K_I (e^{-K_I t} * \hat{p}_s(t)) \right] \\ &- K_I (e^{-K_I t} * (\hat{v}_s - \hat{g}_s)) \end{aligned} \quad (24)$$

where  $\gamma$  and  $\gamma_s$  are constants adjusted for every joint. In order to define the velocity-based variable thresholds for the residuals (4) and (9), the robot dynamics during collision-free periods are considered. Considering that an estimation of  $\tau_{fme}(t)$  and  $\hat{h}(t)$  are available, (13) and (14) are introduced in (12) to obtain a residual signal without systematic modeling inaccuracies. This residual, in the absence of external forces, can be approximated to be zero and is equal to,

$$\hat{r}_c(t) = \hat{r}(t) - \tilde{h}(t) - K_I (e^{-K_I t} * \tau_{fme}) \approx 0 \quad (25)$$

Furthermore, by including  $\tilde{h}(t)$  from (21),

$$\hat{r}_c(t) \approx \hat{r}(t) - \gamma \hat{h}(t) - K_I (e^{-K_I t} * \hat{\tau}_{fme}) \approx 0 \quad (26)$$

In a similar manner, estimations of  $\tau_{sf_e}(t)$  and  $\tilde{h}_s(t)$ , allows to introduce (17), (18) and (23) to obtain the following residual signal,

$$\hat{r}_{s,c}(t) \approx \hat{r}_s(t) - \gamma_s \hat{h}_s(t) + K_I (e^{-K_I t} * \hat{\tau}_{sf_e}) \approx 0 \quad (27)$$

We will use the signals  $\hat{r}_c(t)$  and  $\hat{r}_{s,c}(t)$  to define the velocity-based variant thresholds for the standard residuals  $\hat{r}(t)$  and  $\hat{r}_s(t)$ . To this effect, using the concept of velocity-dependence of friction modeling explained in (19), we obtain the following from (26),

$$L_{\hat{r}}(\dot{q}) < \hat{r}_c(t) < U_{\hat{r}}(\dot{q}) \quad (28)$$

where  $L_{\hat{r}}(\dot{q})$  and  $U_{\hat{r}}(\dot{q})$  are lower and upper bounds of the residual  $\hat{r}_c(t)$ , respectively. These bounds should be determined experimentally. Equation (28) yields to,

$$\begin{aligned} L_{\hat{r}}(\dot{q}) &< \hat{r}(t) - \gamma \hat{h}(t) \\ &- K_I (e^{-K_I t} * \hat{\tau}_{fme}(\dot{q})) < U_{\hat{r}}(\dot{q}) \end{aligned} \quad (29)$$

consequently,

$$LT_{\hat{r}}(t) < \hat{r}(t) < UT_{\hat{r}}(t) \quad (30)$$

$$UT_{\hat{r}}(t) = U_{\hat{r}}(\dot{q}) + \gamma \hat{h}(t) + K_I (e^{-K_I t} * \hat{\tau}_{fme}(\dot{q})) \quad (31)$$



Fig. 2: KUKA Light-Weight Robot

$$LT_{\hat{r}}(t) = L_{\hat{r}}(\dot{q}) + \gamma \hat{h}(t) + K_I (e^{-K_I t} * \hat{\tau}_{fme}(\dot{q})) \quad (32)$$

Where  $UT_{\hat{r}}$  and  $LT_{\hat{r}}$  are the velocity-based variant upper and lower thresholds, respectively, for the external torque observer using motor torques  $\hat{r}(t)$  defined in (4).

Likewise, the following holds true for the external torque observer using joint torque sensors  $\hat{r}_s(t)$  defined in (9),

$$LT_{\hat{r},s}(t) < \hat{r}_s(t) < UT_{\hat{r},s}(t) \quad (33)$$

$UT_{\hat{r},s}$  and  $LT_{\hat{r},s}$  are the upper and lower velocity-based variant thresholds for  $\hat{r}_s(t)$ , respectively, and are equal to,

$$UT_{\hat{r},s}(t) = U_{\hat{r},s}(\dot{q}) + \gamma_s \hat{h}_s(t) - K_I (e^{-K_I t} * \hat{\tau}_{se}(\dot{q})) \quad (34)$$

$$LT_{\hat{r},s}(t) = L_{\hat{r},s}(\dot{q}) + \gamma_s \hat{h}_s(t) - K_I (e^{-K_I t} * \hat{\tau}_{se}(\dot{q})) \quad (35)$$

Similar to (28),  $L_{\hat{r},s}(\dot{q})$  and  $U_{\hat{r},s}(\dot{q})$ , determined experimentally, are lower and upper bounds of the residual  $\hat{r}_{s,c}(t)$  in (27).

Constant thresholds are often used for the purpose of collision detection [9], [10]. Our proposed thresholds (31), (32), (34), and (35) are velocity-dependent in terms of  $\hat{\tau}_{se}(\dot{q})$  and  $\hat{\tau}_{fme}(\dot{q})$ , and time-variant in terms of  $\hat{h}(t)$  and  $\hat{h}_s(t)$ . These variable thresholds result in more true-positive outcomes in collision detection.

## V. CASE STUDY

In this section, our proposed methodology for improving collision detection using velocity-based thresholds for external torque observers described in section IV is examined on a KUKA-LWR robot shown in Fig. 2.

### A. KUKA-LWR Considerations

It must be noted that KUKA-LWR is a flexible joint robot, which is modeled as,

$$M_s(q)\ddot{q} + C_s(q, \dot{q})\dot{q} + g_s(q) = \tau_L + \tau_d + \tau_c - \tau_{frL} \quad (36a)$$

$$B\ddot{\theta} + DK^{-1}\dot{\tau}_s + \tau_s = \tau_m - \tau_{frm} \quad (36b)$$

$$\tau_L = DK^{-1}\dot{\tau}_s + \tau_s \quad (36c)$$

where  $\tau_m$  is the controlled motor torque,  $B$  is the motor inertia matrix,  $\theta$  is the motor position,  $K$  is the diagonal joint stiffness matrix,  $D$  is the diagonal joint viscosity matrix,

$\tau_s = K(\theta - q)$  is the elastic torque measured by the torque sensors,  $\tau_{frm}$  is the friction torque from the motors,  $\tau_{frL}$  is the friction torque from the links, and  $\tau_L$  is the torque transferred to the manipulator's links. By replacing  $\tau_m$  and  $\tau_{fr}$  with  $\tau_L$  and  $\tau_{frL}$ , respectively, all of the equations in sections II-IV become valid for the flexible joint model (36). Therefore, the velocity-based variable thresholds (30-35) are valid for flexible joint robots.

KUKA-LWR employs a state-of-the-art internal feedback loop from the torque sensors to the input motor torque which successfully lowers the effective motor friction  $\tau_{frm}$  and the effective motor inertia  $B\ddot{\theta}$  [9]. The details of this internal feedback loop proposed in [9] are repeated here,

$$\tau_m = BB_\theta^{-1}u + (I - BB_\theta^{-1})\tau_s + (D - BB_\theta^{-1}D_s)K^{-1}\dot{\tau}_s \quad (37)$$

where  $B_\theta$  and  $D_s$  are chosen arbitrarily by the KUKA-LWR controller, and  $u$  is the torque command. Readers are encouraged to refer to [9] for further information. This controller is mentioned here since torque sensor reading errors in (37) will affect the controller motor torque  $\tau_m$  and thereby  $\tau_L$  and the velocity-based thresholds.

Considering (37), (36b), and (36c), the transferred torque to the links  $\tau_L$  is,

$$\tau_L = u - B_\theta\ddot{\theta} - BB_\theta^{-1}\tau_{frm} + (D - D_s)K^{-1}\dot{\tau}_s \quad (38)$$

However, considering torque sensor errors  $\tilde{\tau}_s$ , (38) becomes,

$$\begin{aligned} \tau_L = & u - B_\theta\ddot{\theta} - B_\theta B^{-1}\tau_{frm} + (D - D_s)K^{-1}\dot{\tilde{\tau}}_s \\ & + (B_\theta B^{-1} - I)(\tilde{\tau}_s + DK^{-1}\dot{\tilde{\tau}}_s) \end{aligned} \quad (39)$$

Torque sensors in KUKA-LWR must be calibrated. An inaccurate calibration results in a constant bias. Considering this constant bias in torque sensor readings, and assuming a small  $B_\theta$ ,

$$\tau_L \approx u + (B_\theta B^{-1} - I)\tilde{\tau}_s \quad (40)$$

The biases in the results of the next section are justified by (40). In our experiments, the Fast Research Interface (FRI) module of KUKA-LWR is used to control the robot.

### B. Parameter Adjustment of the Velocity-Based Variable Thresholds

The adjustment of  $\gamma$ ,  $L_{\hat{r}}(\dot{q})$  and  $U_{\hat{r}}(\dot{q})$  and the measurement of  $\hat{\tau}_{fme}(\dot{q})$  in equations (31) and (32) can be done simultaneously. Similarly, the adjustment of  $\gamma_s$ ,  $L_{\hat{r},s}(\dot{q})$  and  $U_{\hat{r},s}(\dot{q})$  and the measurement of  $\hat{\tau}_{se}(\dot{q})$  in equations (34) and (35) can be done simultaneously. To this effect, two least square problems based on (26) and (27) must be used to adjust the proposed variable thresholds parameters. These two least square problems are given here,

$$\min_{\gamma, \hat{\tau}_{fme}(\dot{q})} \left\{ \gamma \hat{h}(t) + K_I (e^{-K_I t} * \hat{\tau}_{fme}(\dot{q})) - \hat{r}(t) \right\} \quad (41)$$

$$\min_{\gamma_s, \hat{\tau}_{se}(\dot{q})} \left\{ \gamma_s \hat{h}_s(t) + K_I (e^{-K_I t} * \hat{\tau}_{se}(\dot{q})) - \hat{r}_s(t) \right\} \quad (42)$$

For the motor torque residual in (30), for every set of collision free data, the least square solution to (41) can be

TABLE I: Estimated  $\gamma \approx \gamma_s$  for All Joints of KUKA-LWR

Joint	$\gamma$
1	0.002
2	$5.06 \times 10^{-4}$
3	0.005
4	0.001
5	-0.0054
6	0.0188
7	-0.0592

used to determine the values of  $\gamma$  and  $\hat{\tau}_{fme}(\dot{q})$ .  $L_{\hat{r}}(\dot{q})$  and  $U_{\hat{r}}(\dot{q})$  can be found by the maximum error for each velocity in the least square solution to (41). A similar method can be used to determine  $\gamma_s$ ,  $\hat{\tau}_{se}(\dot{q})$ ,  $L_{\hat{r}_s}(\dot{q})$ , and  $U_{\hat{r}_s}(\dot{q})$  in (33-35) from (42). Also, the internal feedback loop (37) of the KUKA-LWR controller selects the effective motor inertia  $B_\theta$  as a small value. Therefore, the following holds true for the KUKA-LWR robot,

$$M(q) \approx M_s(q) \implies \begin{cases} \gamma \approx \gamma_s \\ h(t) \approx h_s(t) \end{cases} \quad (43)$$

In order to obtain the data required for formulating the least-square problems of (41) and (42), fifth-order-polynomial trajectories between random set points were followed in the absence of any collisions and values of  $\hat{h}(t)$ ,  $\hat{r}(t)$ ,  $\hat{h}_s(t)$ ,  $\hat{r}_s(t)$  were calculated. Moreover, the values of  $\dot{q}$  were quantized with the resolution of 0.06 Rad/Sec.

The values of  $\hat{\tau}_{fme}(\dot{q})$ ,  $\hat{\tau}_{se}(\dot{q})$ , and  $\gamma \approx \gamma_s$  are obtained from these experiments for all seven joints of the KUKA-LWR robot by solving the least square problems (41) and (42). Fig. 3 shows the results of  $\hat{\tau}_{fme}(\dot{q})$  and  $\hat{\tau}_{se}(\dot{q})$ . The graphs of Fig. 3 have biases that are explained by (40). The values of  $\gamma \approx \gamma_s$  are given in TABLE I.

It should be noted that the data provided in this paper from KUKA-LWR depends on the calibration of the robot and is subject to change if a different robot is used. However, the methodology to calculate the velocity-based thresholds remains unchanged for any manipulator with or without joint torque sensors. In the next section, we compare the proposed thresholds to the constant thresholds.

### C. Comparison of Velocity-Based variable Thresholds with Constant Thresholds

In this section, collision detection of external torque observers, defined in (5) and (10), using proposed velocity-based variable thresholds is compared to collision detection using constant thresholds. In order to demonstrate the performance of the proposed thresholds, random external impact forces were applied by colliding a person's forearm with the second joint of the robot while the robot was following random fifth order polynomial trajectories. The torque sensor-based residuals  $\hat{r}_s(t)$  and their respective velocity-based thresholds were calculated. The results for joints 1-3 are shown in Fig. 4. Motor torque-based residuals  $\hat{r}(t)$  and their velocity-based thresholds for joints 1-3 are also shown in Fig. 5. Similar results were obtained for joints 4-7 which are not included for the sake of brevity. TABLE II compares the time elapsed after collisions and before the detection

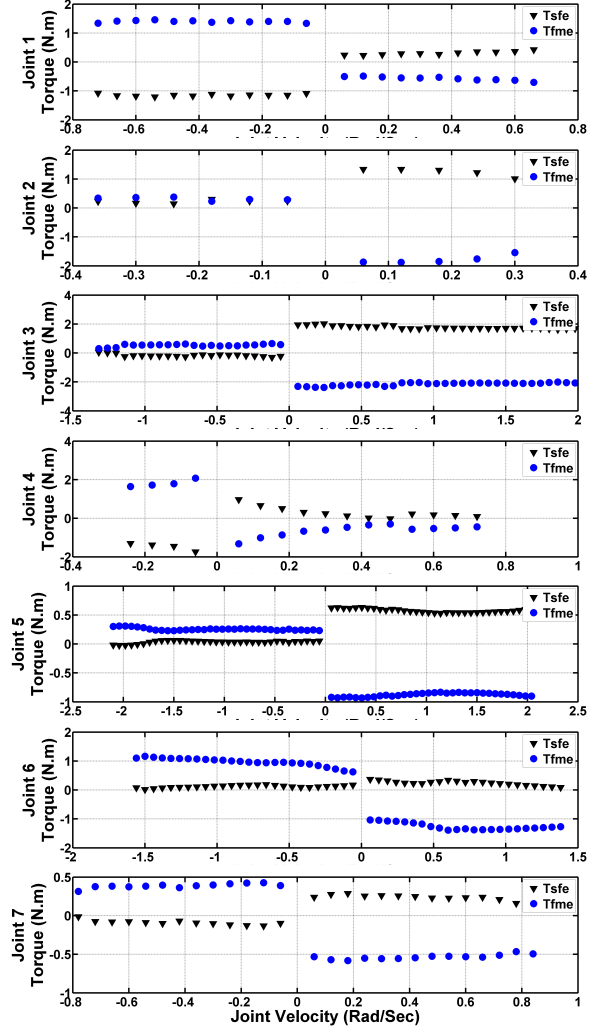


Fig. 3: Estimated values of  $\hat{\tau}_{se}(\dot{q})$  and  $\hat{\tau}_{fme}(\dot{q})$  for all joints of KUKA-LWR

of the collisions for the four thresholds using all seven joints during the same experiment. The results of TABLE II underscore the importance of the proposed velocity-based thresholds in collision detection.

## VI. CONCLUSION

In this paper we examined external torque residuals for serial link manipulators. The accuracy of these residuals for the purpose of collision detection was assessed and a new velocity-based variable threshold for detecting collisions using the residuals was proposed. It was shown that velocity-based variable thresholds, defined based on modeling error and torque sensor inaccuracies, result in more accurate collision detection than constant thresholds. Experimental results validated that the proposed thresholds improve collision detection ability of the external torque observers.

## REFERENCES

- [1] K. Ikuta, H. Ishii, and M. Nokata, "Safety evaluation method of design and control for human-care robots," *International Journal of Robotics Research*, vol. 22, no. 5, pp. 281–297, May 2003.

TABLE II: Collision Detection Times with and without using Velocity-Based Thresholds in KUKA-LWR

Collision Count	Velocity-Based Threshold, Time of Detection (Sec) Using $\hat{r}_s$	Constant Threshold Detection Delay (Sec) Using $\hat{r}_s$	Velocity-Based Threshold, Time of Detection (Sec) Using $\hat{r}$	Constant Threshold Detection Delay (Sec) Using $\hat{r}$
1	2.18	0.02	2.17	0.04
2	4.06	Does Not Detect	4.18	Does Not Detect
3	5.45	0.07	5.54	0.06
4	9.31	0.0	9.63	Does Not Detect
5	11.35	Does Not Detect	11.42	Does Not Detect
6	13.67	0.0	13.73	Does Not Detect
7	16.74	0.0	17.05	Does Not Detect
8	18.70	Does Not Detect	18.46	Does Not Detect
9	20.02	0.0	20.18	0.0
10	23.04	0.0	23.01	0.0
11	26.75	0.04	26.72	0.03
12	30.40	0.16	30.36	Does Not Detect
13	35.57	Does Not Detect	35.53	0.0
14	38.02	0.14	38.05	0.0
15	40.35	0.0	40.39	0.0
16	42.01	0.0	41.94	0.0
17	45.04	0.0	45.22	Does Not Detect
18	46.98	Does Not Detect	47.00	Does Not Detect

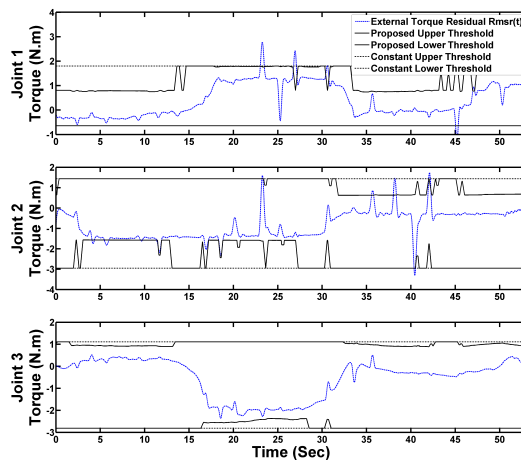


Fig. 4: Torque sensor-based residual  $\hat{r}_s(t)$ , velocity-based variable thresholds, and constant thresholds for joints 1-3 of KUKA-LWR in presence of collision forces

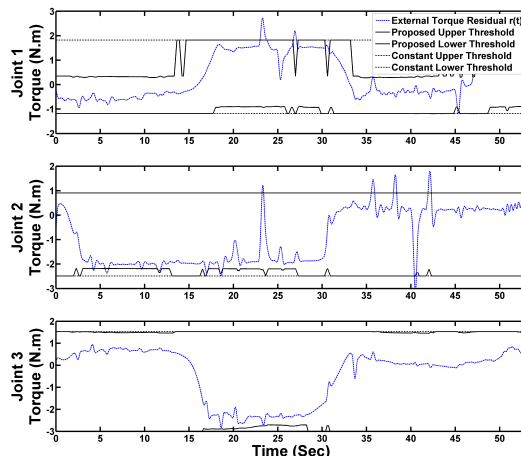


Fig. 5: Motor torque-based residual  $\hat{r}(t)$ , velocity-based variable thresholds, and constant thresholds for joints 1-3 of KUKA-LWR in presence of collision forces

- [2] A. D. Santis, B. Siciliano, A. D. Luca, and A. Bicchi, "An atlas of physical human-robot interaction," *Mechanism and Machine Theory*, vol. 43, no. 3, pp. 253 – 270, 2008.
- [3] A. De Luca, F. Flacco, A. Bicchi, and R. Schiavi, "Nonlinear decoupled motion-stiffness control and collision detection/reaction for the vsa-ii variable stiffness device," in *Intelligent Robots and Systems, 2009. IROS 2009. IEEE/RSJ International Conference on*, 2009, pp. 5487 – 5494.
- [4] A. Pervaz and J. Ryu, "Safe physical human robot interaction-past, present and future," *Journal of Mechanical Science and Technology*, vol. 22, pp. 469–483, 2008.
- [5] S. Katsura, Y. Matsumoto, and K. Ohnishi, "Analysis and experimental validation of force bandwidth for force control," *Industrial Electronics, IEEE Transactions on*, vol. 53, no. 3, pp. 922 – 928, june 2006.
- [6] H. Sneider and P. Frank, "Observer-based supervision and fault detection in robots using nonlinear and fuzzy logic residual evaluation," *Control Systems Technology, IEEE Transactions on*, vol. 4, no. 3, pp. 274 – 282, May 1996.
- [7] W.-H. Chen, D. Ballance, P. Gawthrop, and J. O'Reilly, "A nonlinear disturbance observer for robotic manipulators," *Industrial Electronics, IEEE Transactions on*, vol. 47, no. 4, pp. 932 – 938, Aug. 2000.
- [8] A. Stotsky and I. Kolmanovsky, "Application of input estimation techniques to charge estimation and control in automotive engines," *Control Engineering Practice*, vol. 10, no. 12, pp. 1371 – 1383, 2002.
- [9] A. D. Luca, A. Albu-Schaffer, S. Haddadin, and G. Hirzinger, "Collision detection and safe reaction with the dlr-iii lightweight manipulator arm," in *Intelligent Robots and Systems. 2006 IEEE/RSJ International Conference on*, oct. 2006, pp. 1623 –1630.
- [10] S. Morinaga and K. Kosuge, "Collision detection system for manipulator based on adaptive impedance control law," in *Robotics and Automation, 2003. Proceedings. ICRA '03. IEEE International Conference on*, vol. 1, sept. 2003, pp. 1080 – 1085 vol.1.
- [11] S. Takakura, T. Murakami, and K. Ohnishi, "An approach to collision detection and recovery motion in industrial robot," in *Industrial Electronics Society, 1989. IECON '89., 15th Annual Conference of IEEE*, nov 1989, pp. 421 –426 vol.2.
- [12] C. Canudas de Wit, H. Olsson, K. Astrom, and P. Lischinsky, "A new model for control of systems with friction," *Automatic Control, IEEE Transactions on*, vol. 40, no. 3, pp. 419 –425, mar 1995.
- [13] V. Sotoudehnejad, A. Takhmar, M. Kermani, and I. Polushin, "Counteracting modeling errors for sensitive observer-based manipulator collision detection," in *Intelligent Robots and Systems (IROS), 2012 IEEE/RSJ International Conference on*, oct. 2012, pp. 4315 –4320.